

UNIVERSITAT AUTÒNOMA DE BARCELONA

MASTER IN HIGH ENERGY PHYSICS, ASTROPHYSICS &
COSMOLOGY

MASTER THESIS

An exploratory analysis of broad Kaluza-Klein gluons

Author:

Mikel Mendizabal

Supervisors:

Rafel Escribano

Mariano Quirós

August 31, 2019



**Universitat Autònoma
de Barcelona**

Acknowledgements

I would like to thank my supervisors Mariano Quirós and Rafel Escibano for their guidance throughout the work, I appreciate the extended discussions in our meetings.

I would like to acknowledge Aurelio Juste for the help given in the understanding of the experimental point of view of our work.

Finally, Aitor, Anton and Jon for the long hours of studies, moral support and happy distractions.

An exploratory analysis of broad Kaluza-Klein gluons

M. Mendizabal^a

Supervisors: R. Escribano^{a,b}, M. Quirós^a

^a*Universitat Autònoma de Barcelona, Institut de Física d'Altes Energies (IFAE) and
The Barcelona Institute of Science and Technology (BIST),
Campus UAB, 08193 Bellaterra (Barcelona) Spain*

^b*Grup de Física Teòrica (Departament de Física), Universitat Autònoma de Barcelona,
E-08193 Bellaterra (Barcelona), Spain*

Abstract

All proposed solutions to the hierarchy problem involve new physics at the TeV scale, which stays elusive from experimental searches. One of the most appealing solutions to the hierarchy problem involve a warped extra dimension, with a composite Higgs which melts at a scale of order of few TeV, while the Planck and TeV scale are related by the warp factor along the extra dimension. A theory with a warped extra dimension, and SM bulk propagating fields, contains zero modes, or four-dimensional Standard Model fields, and towers of massive KK resonances. The coupling of these KK resonances to fermions depend on the localization of fermions along the extra dimension. As it turns out that heavy fermions (e.g. the top quarks) are the most massive fermions in the Standard Model, their coupling to KK resonances is the strongest one and the corresponding resonances are then naturally broad, with large values of Γ/M where Γ is the width and M the mass of the resonance.

Out of all KK modes, the KK gluons, with QCD coupling, are the most strongly coupled resonances and can have the largest decay widths. Moreover the QCD sector is, to a large extent, model independent as it does not depend on the details of the electroweak symmetry breaking mechanism. Thus in this work we will explore the possibility that the elusiveness of KK gluons at the LHC arises from the fact that they are sufficiently broad resonances, as the experimental bounds are mainly based on the search of bumps for narrow (isolated) resonances, and they deteriorate whenever the ratio of Γ/M increases. We have then analyzed the pole values of the mass and decay width for broad resonances, and its relation with their renormalized values. We then apply those general results to the particular case of a KK gluon strongly coupled to the top quark and see how the effect of broad resonances affect the prediction for the cross-section times branching ratio both at the partonic and proton level. The more detailed comparison at the proton level with LHC experimental bounds is in progress.

Contents

1	Introduction	1
2	Extra Dimensions	5
2.1	Equations of Motion and Boundary Conditions	5
2.1.1	Real scalar field	6
2.1.2	Fermion fields	7
2.1.3	Gauge fields	8
2.2	Kaluza-Klein decomposition	10
2.2.1	Scalar field decomposition	10
2.2.2	Fermion field decomposition	11
2.2.3	Gauge field decomposition	13
2.3	Warped Background	15
3	Pole mass and decay width of the KK gluon	19
3.1	Quark loop computation	20
3.2	Resummation and renormalization of $\Pi(q)$	22
3.2.1	Resummation	22
3.2.2	Renormalization: the pole approach	23
4	Production and decay of KK gluons: partonic level	29
5	KK gluons in proton-proton collisions	33
5.1	Building the Kaluza-Klein gluon model	33
5.2	Hadronic cross-section	34
6	Summary and outlook	37

1 Introduction

In 1921 the German physicist Theodor Kaluza [1] introduced an extra dimension extending the known 3+1 dimensions of Einstein's General Relativity with metric tensor $g_{\mu\nu}$ ($\mu = 0, 1, 2, 3$) to gravity in 4+1 dimensions with metric tensor g_{MN} ($M = \mu, 5$). With this extension he realized that the five-dimensional (5D) General Relativity contained the four-dimensional (4D) gravity and electromagnetism structure: in fact the 15 independent components of the symmetric tensor g_{MN} split into the 10 independent components of the four-dimensional symmetric tensor $g_{\mu\nu}$, the components $g_{\mu 5}$ are identified with the 4 components of the electromagnetic field, while the remaining component g_{55} is identified with a scalar field, the radion. Six years later, in 1926, Oskar Klein [2] introduced the hypothesis that the fifth dimension is compactified and microscopic. This idea remained till present times and make those theories, the so-called Kaluza-Klein (KK) theories, phenomenologically appealing, while the radion field plays a role in stabilizing the size of the extra dimension. However, the Kaluza-Klein theory breaks down when describing the Standard Model. The failure is partly due to the fact that the fermions that arise from the Kaluza-Klein theory are vector-like, while in the Standard Model they are chiral.

Later on, twenty years ago, in 1999, Lisa Randall and Raman Sundrum (RS) [3] proposed the existence of a *warped* extra dimension (y in proper coordinates) to solve the hierarchy problem. In their approach with a non-flat metric $ds^2 = e^{-A(y)}\eta_{\mu\nu}dx^\mu dx^\nu - dy^2$ with $A(y) = ky$ (k is a constant of the order of the Planck scale related to the AdS_5 curvature), the Planck ($M_P = 2.4 \times 10^{18}$ GeV) and TeV ($M_T \simeq 1$ TeV) scales are related by the warp factor. The 5D theory is Anti de Sitter (AdS_5) and the fifth dimension is compactified, on the interval between the Planck (or ultraviolet (UV)) brane (at $y = 0$ with, conventionally, $A(0) = 0$) and the TeV (or infrared (IR)) brane ($y = L$), which explicitly and spontaneously, respectively, break the conformal invariance of the AdS_5 theory. In this way given that

$$M_T = e^{-A(L)} M_P$$

the hierarchy problem is solved provided that the brane distance is stabilized with $A(L) \simeq 35$. This can be done, as first realized by Goldberger and Wise [4], by introducing a scalar bulk field ϕ with brane potentials explicitly breaking the conformal invariance and fixing the vacuum expectation value $\langle\phi\rangle$ at fixed values ϕ_0 and ϕ_1 at the UV and IR branes.

In this work we will consider an RS 5D theory with all fields (graviton, radion, gauge bosons, fermions, and the scalar Higgs doublet) propagating in the bulk of the extra dimension. All fields have a SM-like zero mode and a discrete tower of massive KK modes. Although 5D fermions are Dirac (vector-like), the problem of chirality is

solved because the extra dimension has the structure of a \mathbb{Z}_2 orbifold and the different boundary conditions for the left-handed and right-handed components prevent the appearance of one chirality at the level of zero modes, while massive KK modes keep the 5D Dirac structure. The different 5D fermions (f) can be given different 5D Dirac masses (characterized by a real constant c_f), which trigger different localization of the corresponding zero mode along the extra dimension. The localization is strongly related to the 5D fermion mass after electroweak symmetry breaking: in particular heavy fermions ($c_f < 1/2$) are strongly localized towards the IR brane while light fermions ($c_f > 1/2$) are localized towards the UV brane. This fact will play a key role in the physics goals of this work as we will see later. Moreover, the zero mode of gauge bosons are flat (constant) along the extra dimensions while their KK modes are strongly localized toward the IR brane. As a consequence, as we will see KK modes are strongly coupled to heavy quarks (just because there is a strong overlapping of their 5D wave functions) and weakly coupled to light fermions (as the wave function overlapping is small).

In the considered RS theory there is a strong contribution of KK modes to electroweak observables which triggers a strong tension with precision experimental data. One proposed way out was enlarging the SM gauge structure $SU(3) \otimes SU(2)_L U(1)_Y$ to $SU(3)_c \otimes SU(2)_L \otimes SU(2)_R \otimes U(1)_{B-L}$ where $SU(2)_R \otimes U(1)_{B-L}$ is broken in the UV brane to $U(1)_Y$ by boundary conditions and unbroken at the IR brane [5]. In this theory the Higgs is a scalar “mesonic” doublet propagating in the bulk and the mechanism of electroweak breaking is similar to that of the SM by means of a Higgs potential localized at the IR brane, but the custodial symmetry remaining on the IR brane protects the theory from large corrections to the electroweak observables. However one can improve over this scheme and enlarge the $SU(2)_L \otimes SU(2)_R \otimes U(1)_{B-L}$ gauge factor to a more general group \mathcal{G} broken at the UV (IR) brane to a subgroup $\mathcal{H}_{UV(IR)}$ and such that the fifth component of the gauge field in the coset $\mathcal{G}/\mathcal{H}_{IR}$ plays the role of the Higgs that will break the electroweak symmetry [6]. In this case the electroweak breaking is triggered by radiative corrections and it is very predictive, while the theory predict the existence of new (heavy) quark zero modes corresponding with the higher dimensionality of the bulk gauge group. The 4D theories dual to these models are dubbed composite Higgs models. For review papers, where details can be found, see e.g. Refs. [7, 8]. Note that the QCD $SU(3)$ subgroup is the same in all these constructions and it is, in this way, pretty model independent.

In this work we will then concentrate in the $SU(3)$ components of these theories. They have 5D gluons in the adjoint $\underline{8}$ representation of $SU(3)$ while the quarks(antiquarks) are in the fundamental $\underline{3}$ (antifundamental $\bar{\underline{3}}$) representation. The 5D gluon has a massless zero mode and massive KK modes. The massless gluon g , which is the SM gluon,

couples to other gluons and to colored fermions with a coupling constant g_s , whose value has been measured to be at the scale $\mu = m_Z$ as $\alpha_s = g_s^2/(4\pi) \simeq 0.118$. However the KK gluons, which are localized toward the IR brane, are coupled to fermions with a strength given by $g_s g_f(c_f)$ where $g_f(c_f)$ is an overlapping integral of the 5D profiles of the gluon KK mode and the zero mode fermions. In this work we will concentrate in the first gluon KK mode ($G^{(1)} \equiv G$) with mass M , which is the lightest KK mode and so can most easily be produced at the LHC. For values of $c_f < 1/2$ we have that $g_f(c_f) \simeq -0.2$, which makes the coupling of G to light fermions very weak, while $g_f(c_f)$ increases for $c_f > 1/2$ as we will see in Fig. 3.

As we can see from Fig. 3, the coupling of G to fermions localized toward the IR brane ($c_f < 1/2$) can be very strong making the decay width $\Gamma(G \rightarrow \bar{f}f)$ large and then possibly the ratio $r = \Gamma/M$ large. In view of the elusiveness of signals in experimental searches at the LHC, we will propose that signals of new physics should come with large values of the parameter r , as experimental bounds deteriorate for large values of r . We will argue that this situation is natural for theories with warped extra dimensions in the presence of heavy fermions which are naturally localized toward the IR brane and with strong couplings to gauge KK modes. Although this statement applies to any gauge KK mode, we will restrict ourselves to the case of gluons because:

1. Gluons are more strongly coupled to fermions than electroweak gauge bosons.
2. As we have explained above, gluons are very model independent since they do not depend on the particular mechanism of electroweak breaking.

The contents of this work are as follows. In Sec. 2 we will provide a brief introduction to the theories with a warped extra dimension which we will use for our analysis. We will pay particular attention to theories where the KK mode G^* is a broad resonance. In Sec. 3 we will study the renormalization effects by which, for a broad resonance, the pole mass and pole width significantly depart from their corresponding renormalized values. We will show that this effect should be thoroughly considered for the relevant cases of broad resonances. The issue of perturbativity, relevant for the case of strongly coupled interactions, is studied in Sec. 4. Cross sections at the partonic and protonic levels will be analyzed in Secs. 5 and 6 respectively. Finally the conclusions and outlook are presented in Sec. 7.

2 Extra Dimensions

In this section we are going to review the properties of a theory with one extra dimension. A cartoon of a slice of the extra dimension between the two branes is represented in Fig. 1, which is a naive representation of the extra dimension. We can distinguish two main types of fields at this stage: i) On one hand, fields that are only allowed to propagate in one of the branes. This is an extreme (limiting) case of a field propagating in the bulk but extremely localized toward the corresponding brane. ii) On the other hand, fields that propagate in the bulk: bulk fields. This extra dimension is defined as

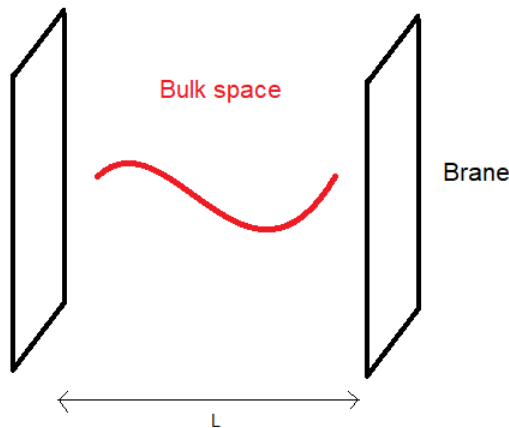


Figure 1: Naive structure of the extra dimension, with length L .

a finite interval and can be considered as a compactified dimension on a circle (S^1) or an orbifold (S^1/\mathbb{Z}_2). Hence, we need to find suitable boundary conditions for the fields.

In addition, our extra dimensional model needs chiral fermions and interactions. The chirality of the theory will allow us to make connections with the Standard Model. The first step is finding appropriate equations of motion and boundary conditions for different kind of fields: scalar, fermionic and gauge boson fields. It is important to point out that in our work we will be working with a warped extra dimension. Thus, the fifth dimension will not be flat.

2.1 Equations of Motion and Boundary Conditions

We first need to describe the geometry of our extra dimension. In general we can define the interval as

$$ds^2 = g_{MN}dx^M dx^N = e^{-2A(y)}\eta_{\mu\nu}dx^{\mu\nu} - dy^2, \quad (2.1)$$

here y defines the proper coordinate of the fifth dimension ¹ which, from Fig. 1, is defined in the interval $y \in [0, L]$. The function $A(y)$ gives us information about the geometry of the extra dimension. If $A(y) = \text{constant}$, the extra dimension is flat. If $A(y)$ is not constant it is wrapped. We start the discussion with a real scalar field.

2.1.1 Real scalar field

The most general action for a real scalar field is given by

$$S = \int d^5x \sqrt{g} \left\{ \frac{1}{2} g^{MN} \partial_M \Phi \partial_N \Phi - \frac{1}{2} M^2 \Phi \right\} \quad (2.2)$$

where $\sqrt{g} = \sqrt{\det(g^{MN})}$ and

$$g^{MN} = \begin{bmatrix} e^{-2A(y)} & & & & \\ & -e^{-2A(y)} & & & \\ & & -e^{-2A(y)} & & \\ & & & -e^{-2A(y)} & \\ & & & & -1 \end{bmatrix}. \quad (2.3)$$

Our goal is to compute a surface term from the action in order to get boundary conditions.

The first step is to derive the equation of motion of our action. We make use of the variational method:

$$\frac{\partial \mathcal{L}}{\partial \Phi} - \partial_M \left(\frac{\partial \mathcal{L}}{\partial (\partial_M \Phi)} \right) = 0. \quad (2.4)$$

We impose a variation in Φ that will affect the action in Eq. (2.2),

$$\delta S = - \int d^5x \left\{ \sqrt{g} M^2 \Phi + \partial_M [\sqrt{g} g^{MN} \partial_N \Phi] \right\} \delta \Phi \quad (2.5)$$

This variation of the action contains a volume term. Thus, if we integrate we can get a surface term that will help to find boundary conditions. However, first we are writing this volume term in our background.

$$\int d^4x \int_0^L dy \{ e^{2A} \partial_\mu \partial^\mu \Phi - e^{4A} \partial_y (e^{-4A} \partial_y \Phi) + M^2 \Phi \} \quad (2.6)$$

Now we can integrate by parts over the extra dimension. After the integration we recover the volume term and a surface term arises,

$$\delta S_s = - \int d^4x e^{-4A} \partial_y \Phi \delta \Phi \Big|_{y=0}^{y=L}. \quad (2.7)$$

¹We will sometimes be using the notation $x^5 \equiv y$ for the fifth dimension.

From this surface term the aforementioned boundary conditions can be derived. The variational method imposes that the expressions above must vanish, $\delta S = \delta S_s = 0$. As we stated before, from Eq. (2.5) we get the equation of motion,

$$e^{2A}\partial_\mu\partial^\mu\Phi - e^{4A}\partial_y(e^{-4A}\partial_y\Phi) + M^2\Phi = 0. \quad (2.8)$$

From the surface term we get the next relation

$$e^{-4A}(\partial_y\Phi\delta\Phi(L) - \partial_y\Phi\delta\Phi(0)) = 0 \quad (2.9)$$

and we find several options: $\Phi = 0$ in the boundaries, $(-)$, or $\partial_y\Phi = 0$ at the limits, $(+)$. Which are, respectively, the so called Dirichlet and Neumann boundary conditions. Moreover, we can combine these into four possible boundary conditions:

- $\partial_y\Phi|_{y=0} = 0$ and $\partial_y\Phi|_{y=L} \rightarrow (+, +)$
- $\partial_y\Phi|_{y=0} = 0$ and $\Phi|_{y=L} \rightarrow (+, -)$
- $\Phi|_{y=0} = 0$ and $\partial_y\Phi|_{y=L} \rightarrow (-, +)$
- $\Phi|_{y=0} = 0$ and $\Phi|_{y=L} \rightarrow (-, -)$

2.1.2 Fermion fields

For the fermionic fields we will use the same procedure although chirality comes to play. Since we need to describe fermions in five dimensions, we need to define five anticommuting Dirac matrices, as

$$\Gamma^A = (\gamma^\alpha, -i\gamma^5) : \quad \alpha = 0, 1, 2, 3 \quad (2.10)$$

where γ^α are the Dirac matrices in the four dimensional representation and γ^5 has the usual four dimensional representation. The Γ^A matrices satisfy the anti-commuting relation $\{\Gamma^A, \Gamma^B\} = 2\eta^{AB}$. We also define the usual 5D relation $g^{MN} = e_M^A e_N^B \eta_{AB}$. The action for free fermions in five dimensions is given by [7]

$$S_\Psi = \int d^5x \sqrt{g} \left(\frac{i}{2} \bar{\Psi} e_A^M D_M \Psi - \frac{i}{2} (D_M \Psi)^\dagger \Gamma^0 e_A^M \Gamma^A \Psi - M \bar{\Psi} \Psi \right), \quad (2.11)$$

where $D_M = (D_\mu, D_5) = (\partial_\mu - \frac{1}{2}e^{-A}A'\gamma_\mu\gamma_5, \partial_5)$.

We now apply the variational method in the action of a free five dimensional fermion. The equation of motion, under a variation in $\bar{\Psi}$, is

$$[ie^A\gamma^\nu\partial_\nu + (\partial_5 - 2A')\gamma_5 - M] \Psi = 0. \quad (2.12)$$

The surface term, that arises from the integration by parts of the variation,

$$-e^4 \delta \bar{\Psi} \gamma_5 \Psi|_{y=0}^{y=L} = 0. \quad (2.13)$$

Using $P_{R,L} = \frac{1 \pm \gamma_5}{2}$, we can write the above expression in terms of right-handed and left-handed chiralities,

$$e^{-4A} (\partial \bar{\Psi}_L \Psi_R - \partial \bar{\Psi}_R \Psi_L)|_{y=0}^{y=L} = 0 \quad (2.14)$$

In order to see the importance of chirality in this extra dimension we rewrite the equations of motion of the fermions in terms of RH and LH and we split it in two equations:

$$\begin{aligned} ie^A \gamma^\nu \partial_\nu \Psi_L + [(\partial_5 - 2A') - M] \Psi_R &= 0 \\ ie^A \gamma^\nu \partial_\nu \Psi_R - [(\partial_5 + 2A') - M] \Psi_L &= 0 \end{aligned} \quad (2.15)$$

In order for the equations to be satisfied and encompass chirality, we take e.g. $\Psi_L = 0$. Hence, we get that $\partial_5 \Psi_R = (2A' + M) \Psi_R$. From here we get two different boundary conditions,

- $(-) \equiv \Psi_L| = 0$
- $(+) \equiv \Psi_R| = 0$.

Thus, we have four combinations for the boundary conditions:

$$(+, +) \quad (+, -) \quad (-, +) \quad (-, -)$$

2.1.3 Gauge fields

For gauge fields we need a slightly different procedure. We need to take into account the 5D gauge fixing. Thus, apart from the kinetic term we add a gauge fixing term to the action,

$$S_A = \int d^5x \sqrt{g} \left(-\frac{1}{4} g^{MN} g^{KL} F_{MK} F_{NL} \right) + S_{GF}. \quad (2.16)$$

We apply the same procedure, first we write the action in the background metric,

$$S_A = \int d^5x \left(-\frac{1}{4} F_{\mu\nu} F^{\mu\nu} + \frac{1}{2} e^{-2A} \partial_\mu A_5 \partial^\mu A_5 - \partial_5 [e^{-2A} A_5] \partial_\mu A^\mu + \frac{1}{2} e^{-2A} \partial_5 A_\mu \partial_5 A^\mu \right) + S_{GF} \quad (2.17)$$

the next step being to compute the equations of motion and the surface term.

After integrating by parts the above volume term, the surface term that arises is

$$S_S = \int d^4x e^{-2A} A_5 \partial_\mu A^\mu. \quad (2.18)$$

There is a mixing term between the two fields A_μ and A_5 . As a consequence, the gauge fixing term is chosen to cancel the mixing term. In particular we choose

$$S_{GF} = - \int d^5x \frac{1}{2\xi} (\partial_\mu A^\mu - \xi \partial_5 [e^{-2A} A_5])^2. \quad (2.19)$$

We then introduce this result in our action getting rid of the mixing term,

$$S_A = \int d^5x \left(-\frac{1}{4} F_{\mu\nu} F^{\mu\nu} + \frac{1}{2} e^{-2A} \partial_\mu A_5 \partial^\mu A_5 + \frac{1}{2} e^{-2A} \partial_5 A_\mu \partial_5 A^\mu - \frac{1}{2\xi} (\partial_\mu A^\mu)^2 - \frac{1}{2} \xi (\partial_5 [e^{-2A} A_5])^2 \right). \quad (2.20)$$

The last step will consist on applying the variational method for the volume and surface terms. From this computation we will get the equations of motion along with the boundary conditions. However, we need to take into account that for this case there are two field components: A_μ and A_5 . Thus, we need to apply the variational method two times per volume and surface term. The equations of motion are then:

$$\begin{aligned} \{g^{\mu\nu} \partial^\mu \partial^\nu - \left(1 - \frac{1}{\xi}\right) \partial^\mu \partial^\nu\} A_\nu - \partial_5 [e^{-2A} \partial_5 A^\mu] &= 0, \\ \partial_\mu \partial^\mu A_5 - \xi \partial_5^2 [e^{-2A} A_5] &= 0. \end{aligned} \quad (2.21)$$

On the other hand, the surface terms:

$$\begin{aligned} \partial_5 A^\mu - \partial^\mu A_5 &= 0, \\ \xi \partial_5 [e^{-2A} A_5] + \partial_\mu A^\mu &= 0. \end{aligned} \quad (2.22)$$

With all the gathered information, we proceed to choose suitable boundary conditions:

$$(+) \equiv A_5| = 0 \Rightarrow \partial_5 A_\mu = 0 \quad \text{and} \quad (-) \equiv A_\mu| = 0 \Rightarrow \partial_5 [e^{-2A} A_5] = 0$$

. In Consequence, we get four different combinations for the boundary conditions at $y = 0, L$:

$$(+, +) \quad (+, -) \quad (-, +) \quad (-, -)$$

. Depending on the chosen boundary conditions we will get different type of gauge bosons. For example, $(+, +)$ boundary conditions will generate the Standard Model gauge bosons. This will be discussed later on in [section 2.2.3](#)

2.2 Kaluza-Klein decomposition

We need to describe how this extra dimension affects our reality. Through a Fourier-mode decomposition we can divide our five dimensional fields as,

$$\Phi(x^\mu, y) = \frac{e^{\alpha_\Phi \cdot A(y)}}{\sqrt{L}} \sum_n \phi_n(x^\mu) f_n(y). \quad (2.23)$$

where α_Φ is a constant coefficient whose value vary depending on the nature of the field, as we will see later on in this section, $f_n(y)$ are the wave function along the extra dimension and $\phi_n(x^\mu)$ which are the 4D fields. Note that the mass dimension of the 5D field Φ is 3/2 for scalars and gauge bosons, and 2 for fermions, while the mass dimension of the 4D fields ϕ_n is 1 for scalars and gauge bosons, and 3/2 for fermions, and the extradimensional profiles f_n are dimensionless. The ϕ_n fields are called the Kaluza-Klein modes and, as we will see later, we can link them with the Standard Model fields. On the other hand, the function f_n , which are the so-called Kaluza-Klein wavefunctions, will determine the localization of the field in the bulk space. The definition of this two terms will be different for scalar, fermionic and gauge boson fields. Thus, we need to find a right definition for these two terms depending on the field.

2.2.1 Scalar field decomposition

We recover the expression in Eq. (2.8), the equation of motion for a real scalar field in five dimensions. Besides, we take the Kaluza Klein decomposition for modes,

$$\Phi(x^\mu, y) = \frac{e^{A(y)}}{\sqrt{L}} \sum_n \phi_n(x^\mu) f_n(y), \quad (2.24)$$

and plug it in the equation of motion,

$$e^{2A(y)} f_n(y) \partial_\mu \partial^\mu \phi_n - e^{3A} \partial_y [e^{-4A} \phi_n \partial_y (e^A f_n)] + M^2 \phi_n f_n = 0. \quad (2.25)$$

A four dimensional free scalar field satisfies the relation $(\partial_\mu \partial^\mu + m_n^2) \phi_n = 0$. Using this relation we get rid of the space-time dependent term ϕ_n , as

$$-e^{2A(y)} f_n(y) m_n^2 - e^{3A} \partial_y [e^{-4A} \partial_y (e^A f_n)] + M^2 f_n = 0. \quad (2.26)$$

Applying the derivatives with respect to y ², we get that

$$f_n m_n^2 e^{2A} - (f_n'' - 2A' f_n' + A'' f_n - 3A'' f_n) + M^2 f_n = 0. \quad (2.27)$$

²We are using the notation $' \equiv \partial/\partial y$.

This equation is valid for a KK mode with any value of n . Consider then two KK modes with numbers n , as before, and m , therefore satisfying the equation

$$f_m m_m^2 e^{2A} - (f_m'' - 2A' f_m' + A'' f_m - 3A'' f_m) + M^2 f_m = 0. \quad (2.28)$$

Multiplying Eq.(2.26) by $e^{-2A} f_m$ and Eq.(2.27) by $e^{-2A} f_n$, we get

$$\begin{aligned} f_n'' f_m e^{-2A} - 2A' f_n' f_m e^{-2A} + [A'' - 3A'^2 - M^2 + e^{2A} m_n^2] f_n f_m &= 0 \\ f_m'' f_n e^{-2A} - 2A' f_m' f_n e^{-2A} + [A'' - 3A'^2 - M^2 + e^{2A} m_m^2] f_m f_n &= 0. \end{aligned} \quad (2.29)$$

We compute the difference for the two expressions above as

$$\partial_y (e^{-2A} [f_m f_n' - f_n f_m']) + (m_n^2 - m_m^2) f_n f_m = 0. \quad (2.30)$$

Integrating over y a surface term arises from the first term that vanishes. Hence, the second term needs to vanish,

$$(m_n^2 - m_m^2) \int_0^L dy f_m f_n = 0. \quad (2.31)$$

As we mentioned before, we imposed that $m_n \neq m_m$ for different modes. Thus, f_n and f_m need to be orthogonal,

$$\int_0^L dy f_m f_n = L \delta_{nm}. \quad (2.32)$$

So as to see how the Kaluza-Klein decomposition affects the action of scalar field, we introduce Eq. (2.23) into Eq. (2.2),

$$\sum_n \int d^4x \frac{1}{2} \phi_n (-\partial_\mu \partial^\mu - m_n^2) \phi_n. \quad (2.33)$$

We see that this is the 4D action which of course does not depend on the extra dimension, it will only depend on the mass and the definition of ϕ_n . In consequence, we see it is in general necessary to study the equations of motion in order to get interesting results.

2.2.2 Fermion field decomposition

The Kaluza-Klein decomposition for fermions needs to distinguish between left and right chiralities, due to the boundary conditions. Thus, we decompose fields as

$$\Psi_{L,R}(x^\mu, y) = \frac{e^{\frac{3}{2}A(y)}}{\sqrt{L}} \sum_n \psi_{L,R}^{(n)}(x^\mu) f_{L,R}^{(n)}(y) \quad (2.34)$$

We then follow the same procedure as for the case of scalar fields. We introduce the Kaluza-Klein decomposition in the equations of motions, as

$$\begin{aligned} m_n^* e^A f_L^{(n)} &= - \left(\partial_y - \frac{1}{2} A' - M \right) f_R^{(n)} \\ m_n e^A f_R^{(n)} &= \left(\partial_y - \frac{1}{2} A' + M \right) f_L^{(n)} \end{aligned} \quad (2.35)$$

Since the equations of motions should be valid in the boundaries (branes) of the extra dimension, we recover the boundary conditions discussed before for fermions,

$$\begin{aligned} (-) &\equiv f_L^{(n)} = 0 \quad \text{and} \quad \left(\partial_y - \frac{1}{2} A' - M \right) f_R^{(n)} = 0 \\ (+) &\equiv f_R^{(n)} = 0 \quad \text{and} \quad \left(\partial_y - \frac{1}{2} A' + M \right) f_L^{(n)} = 0. \end{aligned} \quad (2.36)$$

However, it will be interesting to study the case of zero-mode fermions. The $n = 0$ modes are defined as $m_0 = 0$ so that they represent massless 4D fermions, getting their mass as in the Standard Model, after electroweak symmetry breaking, by Yukawa interactions with the Higgs field. Thus, in the symmetric phase they are really massless modes. Let us then take the case of $n = 0$,

$$\left(\partial_y - \frac{1}{2} A' + M \right) f_L^{(0)} = 0 \rightarrow f_R^{(0)} = N_R e^{-\frac{1}{2} A(y) + \int_0^L M(y) dy}, \quad (2.37)$$

where N_R is a normalization constant. As stated before $f_{L,R}^{(n)}$ functions give the localization of the field in the extra dimension. In this particularly chosen case $f_R(x)$ corresponds to a right-handed SM 4D spinor (as e.g. the quark t_R) which is massless before electroweak breaking but get a breaking mass by the 4D Yukawa interaction with the Higgs field. On the other hand the 5D Dirac mass $M(y)$ is unrelated with the mass of the corresponding SM fermion, but it is related to the localization of the zero mode along the extra dimension. The fermions also satisfy the same normalization condition as scalars:

$$\int_0^L dy f_n f_m = \sqrt{L} \delta_{nm} \quad (2.38)$$

For $M(y) \propto A'(y)$ we find a special case. Take e.g. the right handed chirality, hence, $(-, -)$ boundary conditions. This choice of boundary conditions makes $N_L = 0$. Taking $M(y) = cA'(y)$, we get

$$f_R^{(0)} = N_R e^{(c-\frac{1}{2})A(y)}. \quad (2.39)$$

In Fig. 2 we show a naive representation of the zero-mode fermions Kaluza-Klein wavefunction $f_{L,R}^{(0)}(y)$, for different values of the parameter c . We see that for values of $c > 1/2$ the fermions are localized in the UV brane, while for $c < 1/2$ they are localized in the IR brane. The localization will affect the mass and the coupling with other particles. The free choice of the parameter c will let us explore different couplings of the fermions to the Kaluza-Klein gluon. Besides, this parameter is responsible of the solution of the hierarchy problem, as it will be explained later the localisation will affect the Higgs boson.

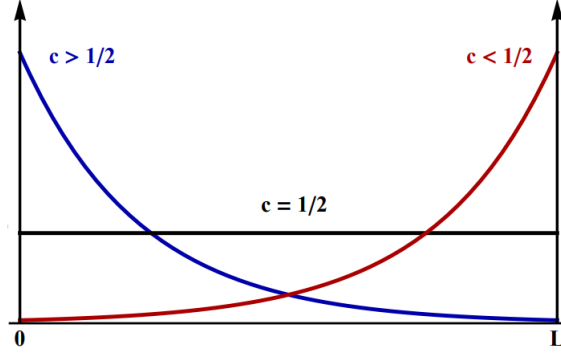


Figure 2: Representation of the Kaluza-Klein wavefunction for the zero-mode fermion $f_{L,R}^{(0)}(y)$ in the extra dimension for different values of the parameter c .

2.2.3 Gauge field decomposition

From the study of the boundary conditions two 5D fields emerged for the gauge bosons: A_μ and A_5 . Thus, they have to be treated separately,

$$A_{\mu,5}(x^\mu, y) = \frac{1}{\sqrt{L}} \sum_n A_{\mu,5}^{(n)}(x^\mu) f_{A,5}^{(n)}(y). \quad (2.40)$$

As done for fermion and scalar fields, we introduce the decomposition in the equations of motions obtained in Sec. 2.1.3. For simplicity we take the Feynman gauge, $\xi = 1$, and obtain

$$\begin{aligned} g^{\mu\nu} A_\nu - \partial_y (e^{-2A} \partial_y A^\mu) &= 0 \Rightarrow m_n^2 f_A^{(n)} + \partial_y (e^{-2A} \partial_y f_A^{(n)}) = 0 \\ \partial_\mu \partial^\mu A_5 - \partial_y^2 (e^{-2A} A_5) &= 0 \Rightarrow m_n^2 f_5^{(n)} + \partial_y^2 (e^{-2A} f_5^{(n)}) = 0 \end{aligned} \quad (2.41)$$

From this relation we are able to link both Kaluza-Klein wavefunctions: $f_5^{(n)}$ and $f_A^{(n)}$, as

$$f_5^{(n)} = \frac{1}{m_n} \partial_y f_A^{(n)}, \quad (2.42)$$

is a solution for the $f_5^{(n)}$ relation, as long as $m_n \neq 0$. It is important to point out that, for $n \neq 0$, $A_5^{(n)}$ provides the longitudinal polarization to its linked massive $A_\mu^{(n)}$.

Recalling the boundary conditions of the gauge bosons in Sec. 2.1.3, we get the boundary conditions concerning the Kaluza-Klein wavefunctions:

$$(+) \equiv \partial_y f_A^{(n)} = f_5^{(n)} = 0; \quad (-) \equiv f_A^{(n)} = 0 \rightarrow \partial_y (e^{-2A} f_5^{(n)})$$

Besides, we normalize the wavefunctions as,

$$\int_0^L dy f_{A,5}^{(n)} f_{A,5}^{(m)} = L \delta_{n,m}. \quad (2.43)$$

Unlike the case of fermions, for the gauge bosons there is no freedom to control their localization in the extra dimension. In the fermion case we introduced the 5D Dirac mass term $M(y)$, that could help to define their localization. However, for gauge bosons there is no such term³. We take the $(+, +)$ boundary conditions for illustration,

$$\partial_y f_A^{(n)} = f_5^{(n)} = 0 \quad \Rightarrow \quad f_A^{(n)} = 1 \quad \text{and} \quad f_5^{(n)} = 0. \quad (2.44)$$

Thus, we see that in both branes f_5 does not have a contribution. However, since $f_A^{(n)} = 1$ we can relate these boundary conditions with spin-1 gauge bosons. In consequence, the 0-modes of these gauge bosons can be linked with the Standard Model spin-1 bosons.

We now discuss the $(-, -)$ boundary conditions in the branes. This case is of interest for models where the fifth component of some gauge field components play the role of the SM Higgs, as in the composite Higgs theories we mentioned in Sec. 1. We find $f_A^{(n)} = 0$. Thus, there is no spin-1 gauge boson. Nonetheless, if we take the 0-mode

$$\partial_y (e^{-2A} f_5^{(0)}) = 0 \Rightarrow f_5^{(0)} = N e^{2A}, \quad (2.45)$$

where N is a normalization constant, we find a scalar gauge boson. This can be associated with the Standard Model Higgs boson. In comparison with the spin-1 field (with flat wavefunction along the extra dimension), the spin-0 gauge boson localization is provided by the background.

³This statement is exact for KK gluons and photons which remain massless after electroweak breaking. For massive gauge bosons, W and Z , one should introduce a 5D mass term which depends on the Higgs VEV and give a mass to all KK modes after electroweak breaking. However, given that the electroweak mass is negligible as compared to the compactification mass of KK modes one usually can neglect this effect in most of the applications. We again stress that in the case of gluons, considered in this work, the statement is strictly correct.

2.3 Warped Background

Until now we used a general background in the study of the fields. However, as discussed in the introduction our work is based in a warped extra dimension. Hence, the spacetime is extremely warped near the IR brane $A(L) \gg 1$. Besides, we need to know at what energy scales the Kaluza-Klein modes are excited. It is given by the warped down curvature at $y = L$,

$$k_{eff} = -\partial_y e^{-A(y)}|_{y=L} = A'(y)e^{-A(y)}. \quad (2.46)$$

Another important parameters to discuss are the couplings, and how they get affected by the extra dimension. Let us suppose an interaction between one gauge boson (say a gluon) and two fermions (say quarks), as

$$\mathcal{L}_{int} \propto g_5 \int_0^L dy e^{-3A(y)} A_\mu(x, y) \bar{\Psi}(x, y) \gamma^\mu \Psi(x, y). \quad (2.47)$$

After introducing the corresponding Kaluza-Klein decomposition for the fields,

$$\mathcal{L}_{int} \propto \sum_{n,m,r} \frac{g_5}{\sqrt{L}} \int_0^L dy \frac{1}{L} f_n(y) f_m(y) f_r(y) A_\mu^n(x) \bar{\psi}_m(x) \gamma^\mu \psi_r(x). \quad (2.48)$$

Thus, in order to have a four dimensional interaction,

$$\mathcal{L}_{int} = g_4^{nmr} A_\mu^n(x) \bar{\psi}_m(x) \gamma^\mu \psi_r(x), \quad (2.49)$$

the four dimensional coupling has to be defined as

$$g_4^{nmr} = g_4 \int_0^L dy \frac{1}{L} f_n(y) f_m(y) f_r(y), \quad g_4 \equiv \frac{g_5}{\sqrt{L}}. \quad (2.50)$$

Moreover, using the normalization of fields, $\int_0^L dy f_n f_m = L \delta_{nm}$, and if we consider the case of a gauge boson zero mode $n = 0$ then by the orthogonality relation, as $f_0(y) = \text{constant}$, then it turns out that the coupling is constrained to the case $n = r$.

In this work we will consider the case of fermion zero modes $m = r = 0$ and the first KK mode of the gauge boson $n = 1$, i.e. g_4^{100} . The corresponding integral is allowed by the orthogonality relations as the profile of zero mode fermions are non-trivial along the extra dimension. Furthermore, the more overlapped the Kaluza-Klein wavefunctions are, the stronger is the coupling, as already anticipated in the introduction.

We will do a small recap in order to discuss the Standard Model in the warped background. We saw that the compactification on the extra dimension is chiral, i.e. it differs between left and right chiralities. Moreover, the localization of the fermions

depends on the free parameter $M(y)$. Thus, we have the freedom to choose the localization of the different SM fermions. However, once the background is set, the gauge fields have a fixed localization in the extra dimension.

These properties help in the understanding of the hierarchy problem. Suppose a five dimensional Yukawa interaction,

$$\mathcal{L}_{int} = y_5 \int_0^L dy e^{-4A} H(x, y) \bar{\Phi}(x, y) \Phi(x, y). \quad (2.51)$$

We only take the zero-modes, i.e. the Standard Model fields, and the previous interaction translates into

$$\mathcal{L}_{int} = \frac{y_5}{L^{3/2}} \int_0^L dy f_H^0(y) f_L^0(y) f_R^0(y) H(x) \bar{\psi}_L(x) \psi_R(x). \quad (2.52)$$

Then, the Standard Model Yukawa coupling Lagrangian as

$$\mathcal{L}_{int} = y_4 H(x) \bar{\psi}_L(x) \psi_R(x) + h.c. \quad (2.53)$$

implies a 4D Yukawa coupling given by

$$y_4 = \frac{y_5}{L^{3/2}} \int_0^L dy f_H^0(y) f_L^0(y) f_R^0(y). \quad (2.54)$$

From the last equation one easily concludes that heavy (light) SM fermions are localized toward the IR (UV) brane. In fact, in order to solve the hierarchy problem, it turns out that the Higgs profile has to be localized toward the IR brane. More in detail, $f_H^0(y) \propto e^{aky}$ with $a \geq 2$ ⁴ which means that the Higgs profile is strongly localized toward the IR brane. As heavy fermions have large 4D Yukawa couplings, their wavefunctions have to overlap a large extent with the Higgs profile, i.e. they have to be localized toward the IR brane, and therefore for them $c < 1/2$. Likewise light fermions have small Yukawa couplings, which are provided by the overlapping integral if their wavefunctions are localized toward the UV brane, i.e. if $c > 1/2$. This explains why KK gauge modes are strongly (weakly) coupled to heavy (light) fermions.

For now on we are using AdS_5 background, $A(y) = ky$, where k is the curvature. Now that the background is set, we can compute the Kaluza-Klein wavefunctions, $f_n(y)$. We start solving the case of the scalar field, with 5D square mass given by $M^2 = (\alpha^2 - 4)K^2$,

$$f_n''(y) - 2kf_n'(y) + (-3k^2 - (\alpha^2 - 4) + e^{2ky}m_n^2) f_n(y) = 0. \quad (2.55)$$

⁴This condition is required by the solution to the hierarchy problem, as a plays the role of the dimension of the Higgs operator \mathcal{O}_H in the 4D dual theory, so that the dimension of the quadratic operator \mathcal{O}_H^2 is $\sim 2a > 4$.

whose solution is the Bessel function

$$f_n(y) = N_n e^{ky} \left\{ J_\alpha \left(\frac{m_n}{k} e^{ky} \right) + b_n Y_\alpha \left(\frac{m_n}{k} e^{ky} \right) \right\}. \quad (2.56)$$

For the case of the fermions, if we set $M = \pm ck$, the solution is

$$f_{L,R}^{(n)} = N_n e^{ky} \left[J_{c \pm \frac{1}{2}} \left(\frac{m_n}{K} e^{ky} \right) + b_n Y_{c \pm \frac{1}{2}} \left(\frac{m_n}{K} e^{ky} \right) \right] \quad (2.57)$$

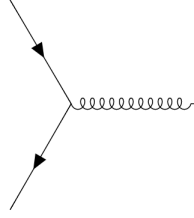
For gauge bosons, without electroweak symmetry breaking, the Kaluza-Klein function also reduces to Bessel functions

$$f_n = N_n e^{ky} \left[J_1 \left(\frac{m_n}{K} e^{ky} \right) + b_n Y_1 \left(\frac{m_n}{K} e^{ky} \right) \right], \quad (2.58)$$

where for the three type of fields N_n is the normalization condition, b_n is set after the IR boundary condition is imposed and m_n is then fixed from the UV boundary condition.

3 Pole mass and decay width of the KK gluon

The interaction between the 5D quark Ψ and the KK gluon G^a is defined by the Lagrangian:



$$\mathcal{L}_{int} \propto -ig_s \bar{\Psi} G_\mu^a \gamma^\mu t^a \Psi \frac{1}{L} \int_0^L f_G^{(1)}(y) f_q^{(0)}(y) f_q^{(0)}(y) dy, \quad (3.1)$$

where g_s is the 4D QCD coupling and we have used the KK-decomposition and normalization conventions from the previous section. We then define the overlapping integral as

$$g_q(c_q) \equiv \frac{1}{L} \int_0^L f_G^{(1)}(y) f_q^{(0)}(y) f_q^{(0)}(y) dy. \quad (3.2)$$

which depends on the localization coefficients of the quark Ψ , c_q . The function $g_q(c_q)$ is plotted in Fig. 3 for the RS metric.

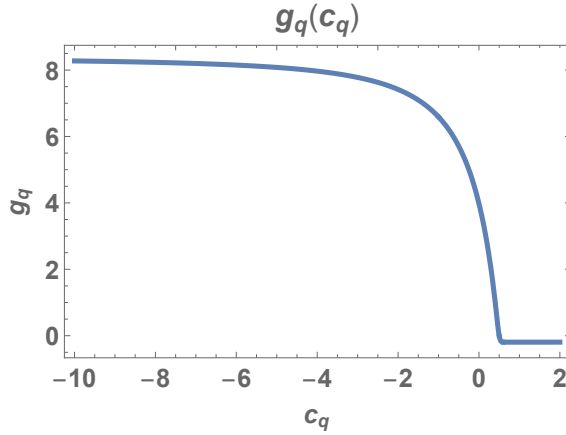


Figure 3: The function $g_q(c_q)$ as a function of the parameter c_q which characterizes the quark q .

We then can write the 4D interaction Lagrangian as

$$\mathcal{L}_{int} \sim -ig_s g_f \bar{\Psi} G_\mu^a \gamma^\mu t^a \Psi \quad (3.3)$$

Our goal is to compute the two point function of the KK gluon with its first correction. We start from the definition of the propagator,

$$\langle 0|TG_\mu(x)G_\nu(0)e^{iS}|0\rangle, \quad (3.4)$$

where S is the action. In order to add the first correction to the propagator, we expand the exponential in terms of the coupling g_0 . The terms we are interested in are

$$\begin{aligned} \langle 0|TG_\mu(x)G_\nu(0)e^{iS}|0\rangle &\simeq G_\mu(x)G_\nu(0) \\ &+ g_0^2 G_\mu(x) \int d^4 z_1 d^4 z_2 : \bar{\Psi} G_\rho^a \gamma^\rho t^a \Psi : (z_1) : \bar{\Psi} G_\sigma^b \gamma^\sigma t^b \Psi : (z_2) G(0) + \dots \end{aligned} \quad (3.5)$$

We contract the fields and rewrite them in momentum space, using the Fourier transform, we get that

$$\begin{aligned} \langle 0|TG_\mu(x)G_\nu(0)e^{iS}|0\rangle &= D_{\mu\nu}^{(0)}(q) \\ &+ i g_0^2 \text{Tr}[t^a t^b] D_{\mu\rho}^{(0)}(q) \int \frac{d^4 k}{(2\pi)^4} \text{Tr}[S(p+k)\gamma^\rho S(k)\gamma^\sigma] D_{\sigma\nu}^{(0)}(q). \end{aligned} \quad (3.6)$$

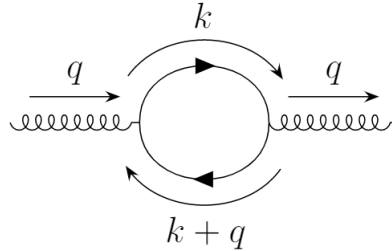
Thus, the propagator of the gluon at first order correction is

$$D_{\mu\nu}^{(1)} = D_{\mu\nu}^{(0)}(q) + D_{\mu\rho}^{(0)}(q) \Pi^{\rho\sigma}(q) D_{\sigma\nu}^{(0)}(q), \quad (3.7)$$

Where $\Pi^{\rho\sigma}(q)$ is the correction due to a quark loop in our case.

3.1 Quark loop computation

From Eq. (3.6) the correction that needs to be computed is the loop in the next diagram



$$\Pi^{\mu\nu}(q) = i g_0^2 \text{Tr}[t^a t^b] \int \frac{d^4 k}{(2\pi)^4} \text{Tr}[S(k+q)\gamma^\mu S(k)\gamma^\nu]. \quad (3.8)$$

In order to solve this equation, we use dimensional regularization. We promote the dimension of our integral 4 to D dimensions, being $D = 4 - 2\epsilon$. As we need to keep dimensionality, we have to add an energy scale μ ,

$$\Pi^{\mu\nu}(q) = ig_0^2 Tr[t^a t^b] \mu^{2\epsilon} \int \frac{d^D k}{(2\pi)^D} \frac{Tr[(\not{k} + \not{q} + m)\gamma^\mu(\not{k} + m)\gamma^\nu]}{[(k+q)^2 - m^2 + i\epsilon][k^2 - m^2 + i\epsilon]}. \quad (3.9)$$

Making use of the Wick rotation, computing the trace and using Feynman parametrization we get:

$$\begin{aligned} \Pi^{\mu\nu}(q) = & ig^2 \mu^{2\epsilon} Tr[t^a t^b] \int_0^1 dx \int \frac{d^D k}{(2\pi)^D} \\ & \times \frac{g^{\mu\nu}(m^2 - q^2 x(1-x)) - (q^\mu q^\nu - q^2 g^{\mu\nu})2x(1-x) + 2k^\mu k^\nu - k^2 g^{\mu\nu}}{k^2 - m^2 + q^2 x(1-x)}. \end{aligned} \quad (3.10)$$

Then, we solve the integral for the momentum k and defining $A = m^2 - q^2 x(1-x)$,

$$\begin{aligned} \Pi^{\mu\nu}(q) = & ig^2 \mu^{2\epsilon} Tr[t^a t^b] \int_0^1 dx \{Ag^{\mu\nu} - (q^\mu q^\nu - q^2 g^{\mu\nu})2x(1-x) - Ag^{\mu\nu}\} \\ & \times \frac{\Gamma(2 - \frac{D}{2})}{(4\pi)^{D/2}} \frac{1}{A^{2-D/2}}. \end{aligned} \quad (3.11)$$

Substituting $D = 4 - 2\epsilon$ and $Tr[t^a t^b] = 1/2$ in the equation we get

$$i\Pi^{\mu\nu}(q) = \frac{2}{(4\pi)^2} g^2 \mu^{2\epsilon} \int_0^1 dx \Gamma(\epsilon) \left(\frac{4\pi\mu^2}{A} \right)^\epsilon (q^\mu q^\nu - q^2 g^{\mu\nu})2x(1-x) \quad (3.12)$$

We can extract the Lorentz structure from the above expression, $\Pi^{\mu\nu}(q) = (q^\mu q^\nu - q^2 g^{\mu\nu})\Pi(q)$, and work with the scalar part. Afterwards, in order to go back to a four dimensional integral we will take the limit $\epsilon \rightarrow 0$. We do a Taylor expansion in ϵ

$$\begin{aligned} i\Pi(q) = & \frac{2}{(4\pi)^2} g^2 \left(\frac{1}{\epsilon} + \gamma_E + \frac{1}{12}\epsilon(6\gamma_E^2 + \pi^2) + \mathcal{O}(\epsilon^2) \right) \\ & \times \int_0^1 dx \left(1 + \epsilon \log \frac{4\pi\mu^2}{A} + \mathcal{O}(\epsilon^2) \right) 2x(1-x) \end{aligned} \quad (3.13)$$

Since $\epsilon \rightarrow 0$, we truncate our expansion in ϵ in $\mathcal{O}(\epsilon)$. Introducing again $A = m^2 - q^2 x(1-x)$,

$$i\Pi(q) = \frac{2}{(4\pi)^2} g^2 \int_0^1 dx \left\{ \frac{1}{\epsilon} - \gamma_E + \log 4\pi + \log \frac{\mu^2}{m^2} - \log \left(1 - x(1-x) \frac{q^2}{m^2} \right) \right\} 2x(1-x). \quad (3.14)$$

We decide to use the \overline{MS} renormalization scheme where the term $1/\widehat{\epsilon} = 1/\epsilon + \gamma_E + \log 4\pi$ is subtracted

$$i\Pi(q) = \frac{2}{(4\pi)^2} g^2 \left\{ \frac{1}{3} \frac{1}{\widehat{\epsilon}} + \frac{1}{3} \log \frac{\mu^2}{m^2} - \int_0^1 dx \left(1 - x(1-x) \frac{q^2}{m^2} \right) \right\} 2x(1-x). \quad (3.15)$$

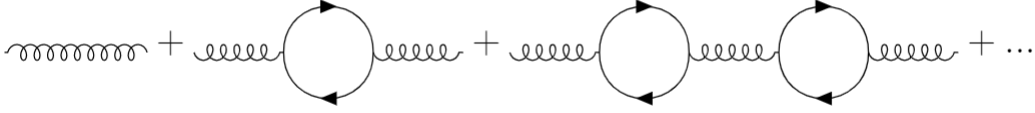
For chiral fermions, as e.g. the case of the quark t_R ⁵ a factor 1/2 arises in the computation of the correction,

$$i\Pi(q) = \frac{1}{(4\pi)^2} g^2 \left\{ \frac{1}{3} \frac{1}{\widehat{\epsilon}} + \frac{1}{3} \log \frac{\mu^2}{m^2} - \int_0^1 dx \left(1 - x(1-x) \frac{q^2}{m^2} \right) \right\} 2x(1-x). \quad (3.16)$$

3.2 Resummation and renormalization of $\Pi(q)$

3.2.1 Resummation

The next step will be to add and resum all 1PI diagrams in



$$D_{\mu\nu}^{(1)}(q) = D_{\mu\nu}^{(0)} + D_{\mu\alpha}^{(0)} \Pi^{\alpha\beta} D_{\beta\nu}^{(0)} + D_{\mu\alpha}^{(0)} \Pi^{\alpha\beta} D_{\beta\gamma}^{(0)} \Pi^{\gamma\xi} D_{\xi\nu}^{(0)} \quad (3.17)$$

where as mentioned D^0 is the massive gluon propagator with a *bare* mass M_0 . Writing the propagator in the unitary gauge, we are going to try to find a pattern in this summation in order to resum,

$$\begin{aligned} D_{\mu\nu}^{(1)} &= i \frac{-g_{\mu\nu} + q_\mu q_\nu / M_0^2}{q^2 - M_0^2} + i \frac{-g_{\mu\alpha} + q_\mu q_\alpha / M_0^2}{q^2 - M_0^2} i (q^2 g^{\alpha\beta} - q^\alpha q^\beta) \Pi(q) i \frac{-g_{\beta\nu} + q_\beta q_\nu / M_0^2}{q^2 - M_0^2} + \dots \\ &= i \frac{-g_{\mu\nu} + q_\mu q_\nu / M_0^2}{q^2 - M_0^2} - i \frac{q^2 g_{\mu\nu} - q_\mu q_\nu}{q^2 - M_0^2} \frac{\Pi(q)}{q^2 - M_0^2} + \dots = \\ &= i \frac{-g_{\mu\nu} + q_\mu q_\nu / q^2}{q^2 - M_0^2} \left(1 + \frac{q^2 \Pi(q)}{q^2 - M_0^2} + \dots \right) + \frac{q_\mu q_\nu}{q^2 - M_0^2} \frac{-M_0^2 + q^2}{M_0^2 q^2}. \end{aligned} \quad (3.18)$$

⁵Notice that, unlike the case of the SM gluon g whose fermion interactions are vector-like, the fermion interactions of the KK gluon G are not vector-like if the wavefunctions of both chiralities f_L and f_R are different.

For an infinite number of 1PI we will have a series related to $\frac{1}{1-x} = 1 + x + x^2 + \dots$; where $x = q^2\Pi(q)/(q^2 - M_0^2)$. Thus, replacing the series with its function we get that the propagator at first order correction is

$$D_{\mu\nu}^{(1)} = i \frac{-g_{\mu\nu} + q_\mu q_\nu / q^2}{q^2 - M_0^2 - q^2\Pi(q)} + q_\mu q_\nu \text{ terms} \quad (3.19)$$

When contracting the KK gluon propagator to a fermion current the $q_\mu q_\nu$ terms vanish (Ward identity). However, we need to remember that the function $\Pi(q)$ is divergent at $\epsilon \rightarrow 0$. In order to get rid of this divergence we need to renormalize the parameters of the $\Pi(q)$ function. In our case the pole approach scheme will be used.

3.2.2 Renormalization: the pole approach

In the pole approach we renormalize the propagator in order to remove the divergences, these divergences are absorbed by counter-terms. Besides, in this approach we are able to relate the denominator of the propagator with the pole mass and the pole decay width of the KK gluon. What we need to do is

$$\frac{i}{q^2 - M_0^2} \rightarrow \frac{i}{s - s_p},$$

where $s = q^2$ and, in a relativistic approximation, $s_p \equiv M_p^2 - iM_p\Gamma_p$, where M_p is the pole mass and Γ_p the pole decay width.

The first step will be getting rid of the divergence of $\Pi(q^2)$. For that we are taking the denominator of the propagator of Eq. (3.19)

$$D(q^2) = q^2 - M_0^2 - q^2\Pi(q^2), \quad (3.20)$$

and define $\hat{\Pi}(q^2) \equiv \Pi(q^2) - \Pi(0)$. With this redefinition $\hat{\Pi}(q^2)$ is no longer divergent, and

$$D(q^2) = q^2 - M_0^2 - q^2 \left(\hat{\Pi}(q^2) + \Pi(0) \right) = q^2 (1 - \Pi(0)) - M_0^2 - q^2 \hat{\Pi}(q^2) \quad (3.21)$$

The mass term has to be renormalized as,

$$M_0^2 = M_R^2 (1 - \Pi(0))$$

where M_R is the (finite) renormalized mass in this renormalization scheme. Moreover, we can approximate $(1 - \Pi(0))\hat{\Pi}(q^2) \simeq \hat{\Pi}(q^2)$. This can be done since the term $\Pi(0)\hat{\Pi}(q^2)$ is a $\mathcal{O}(g^4)$ term and we are working at $\mathcal{O}(g^2)$. These higher order divergences will be absorbed by higher loop corrections. Thus working in the one loop approximation, we can ignore them, leaving the denominator as

$$D(q^2) = (1 - \Pi(0))(q^2 - M_R^2 - q^2\hat{\Pi}(q^2)). \quad (3.22)$$

We now redefine the quark field, so the divergence is absorbed, $\Psi_0 = Z_q^{1/2}\Psi_R$, a wave function renormalization ⁶. Hence, $Z_q^{(1)} = 1 - \Pi(0)$, and the denominator remains as

$$D(q^2) = q^2 - M_R^2 - q^2\hat{\Pi}(q^2). \quad (3.23)$$

We can now relate our denominator with the terms of the Breit-Wigner resonance function for the propagator, having $s_p = M_R^2 + q^2\hat{\Pi}(q^2)$. In consequence, we will be able to compute the pole mass and the pole decay width for a given renormalized mass M_R and gauge coupling g_R . First we need to find a pole value of s which makes the denominator to vanish,

$$D(s) = s - s_p = s - M_R^2 - s\hat{\Pi}(s) \rightarrow D(s_p) = 0. \quad (3.24)$$

Thus, this will happen in general for a complex value $s = s_p$ as the previous equation splits into a real and an imaginary component. Since we use the relativistic definition of s_p , we can find the values of the pole mass and the pole decay width by solving the above system and identifying

$$\begin{aligned} \text{Re}[s_p] &= M_p^2 \\ \text{Im}[s_p] &= M_p\Gamma_p \end{aligned} \quad (3.25)$$

In summary, in the process of renormalization two parameters have been redefined, the mass and the quark field. The quark field redefinition is absorbed in the renormalization of the gauge coupling. Hence, these are the renormalizations:

$$\begin{aligned} M_0^2 &= M_R^2(1 - \Pi(0)), \\ g_0 &= g_R(1 + \Pi(0)). \end{aligned} \quad (3.26)$$

In the previous renormalization process we have been subtracting $\Pi(0)$ which is real, so that we have chosen a reference momentum for the renormalization condition $q^2 = 0$, and called M_R the renormalized mass in this scheme. Alternatively we can choose for the renormalization condition a different momentum q^2 , for instance we can choose the (renormalized) mass itself $q^2 = M^2$ for the renormalization point ⁷. In this case $\Pi(M^2)$ will in general be a complex number so that we have to subtract only its real part for the mass renormalization, and take

$$\hat{\Pi}(q^2) = \Pi(q^2) - \text{Re}[\Pi(M^2)].$$

⁶Ultimately we can absorb this divergence in the renormalization of the gauge coupling constant g .

⁷Notice that, in the one loop approximation we are working, it is equivalent to consider the bare, M_0 , or the renormalized, M , masses for the renormalization point. We are calling M the renormalized mass, and g the renormalized gauge coupling, in this renormalization scheme.

Following the same procedure as before, we reach the same denominator as in Eq. (3.23). However, now the renormalization of the mass and the coupling differ:

$$\begin{aligned} M_0^2 &= M^2(1 - \text{Re}[\Pi(M^2)]), \\ g_0 &= g(1 + \text{Re}[\Pi(M^2)]). \end{aligned} \quad (3.27)$$

We can see that there is a relation between both renormalization schemes:

$$\begin{aligned} M_R^2 &= M^2 \frac{1 - \text{Re}[\Pi(M^2)]}{1 - \Pi(0)} = M^2 (1 - \text{Re}\Pi(M^2) + \Pi(0)), \\ g_R &= g \frac{1 + \text{Re}[\Pi(M^2)]}{1 + \Pi(0)} = M^2 (1 + \text{Re}\Pi(M^2) - \Pi(0)). \end{aligned} \quad (3.28)$$

At the end of the day it does not matter what renormalization scheme we use. Because for different renormalization schemes the pole mass and the pole decay width must be the same. In order to check this explicitly, we have computed the pole mass and pole decay width in two related renormalization schemes for common values of the bare quantities. As an example we have worked out an academic case with extremely large gauge couplings in order to stress possible differences in both schemes. We set $M_p = 2$ TeV and $\Gamma_p = 1$ TeV. For the $q^2 = 0$ renormalization scheme we deduce that $M_R = 3.61$ TeV and $g_R = 15.26$ as renormalized quantities. On the other hand, in the $q^2 = M^2$ renormalization scheme we get $M = 2.22$ TeV and $g = 9.34$ as renormalized quantities. These two results fulfil the relation in Eq. (3.28).

Moreover, it would be interesting to see how the corrections affect a given renormalized mass in both schemes, i.e. the difference between the renormalized and the pole masses. In Fig. 4, we can observe, as in the previous numerical example, that the corrections in the $q^2 = 0$ scheme are bigger. This is due to the definition of $\hat{\Pi}(q^2)$. In the $q^2 = 0$ scheme $\text{Re}\hat{\Pi}(q^2)$ is bigger than in the $q^2 = M^2$ scheme. Since the correction is proportional to $\text{Re}\hat{\Pi}(q^2)$, as we can see in Eq. (3.23), the correction is bigger for $q^2 = 0$. In this plot we name M the renormalized mass in the corresponding renormalization scheme and M_p the corresponding pole mass.

Another good comparison is to see how different values of M are affected in the same scheme. In Fig. 5 we can see that for $q^2 = 0$ the correction shows a dependence in the input mass, M . The higher the mass the bigger the correction. The renormalization at $q^2 = M^2$ shows also dependence in the input mass. However, the corrections are much smaller. This corrections become distinguishable at high values of g .

A very important issue in this discussion should be the validity of perturbation theory in the different renormalization schemes. For that issue we will consider, as was done in the rest of this section, both renormalization schemes at $q^2 = 0$ and

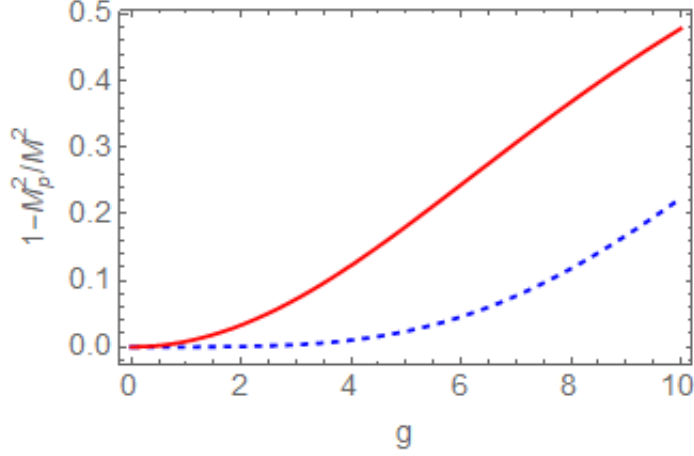


Figure 4: Corrections for M_p for $M = 3\text{TeV}$ and values of g between 0 and 10. Thick red line for renormalization at $q^2 = 0$ and dashed blue for renormalization at $q^2 = M^2$. In both case M and g refer to renormalized quantities.

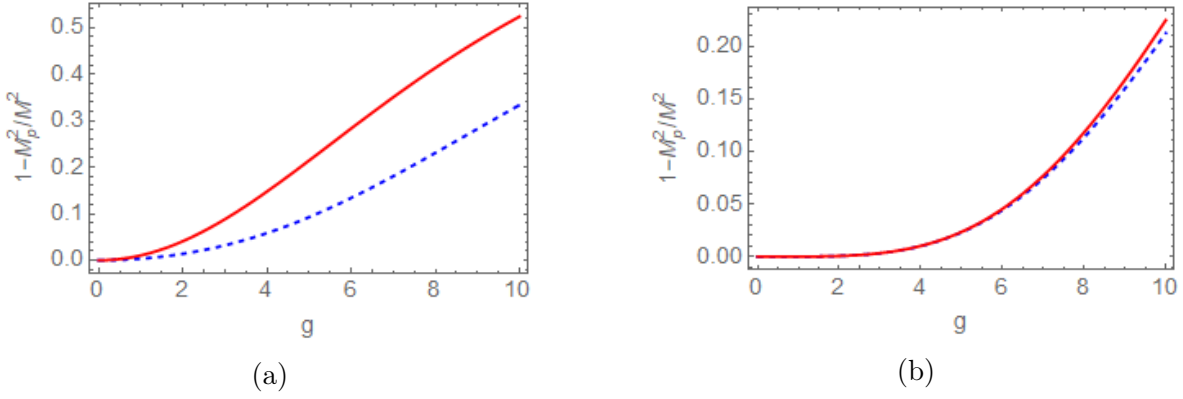


Figure 5: Corrections to the mass: dashed blue line for $M = 1\text{ TeV}$ and red thick line for $M = 5\text{ TeV}$. (a) Renormalization at $q^2 = 0$. (b) Renormalization scheme at $q^2 = M^2$. Here M and g refer to renormalized quantities in both renormalization schemes.

$q^2 = M^2$, where M is in both cases the renormalized mass. We can measure the *degree of perturbativity* p by the quantity

$$p \equiv \frac{\Delta M}{M} = \frac{M - M_p}{M} = 1 - \frac{M_p}{M} \quad (3.29)$$

and its relation with the renormalization scheme in the limit of strong coupling, i.e. in the cases of broad resonances, since it will show us how big the correction to the mass is compared to the input mass. An obvious perturbativity bound would impose $p < 1$ although much stronger constraints could apply from the higher loop study of the given

processes⁸. While keeping the bound $p < 1$ the philosophy in this work would be to work for values of p as small as possible.

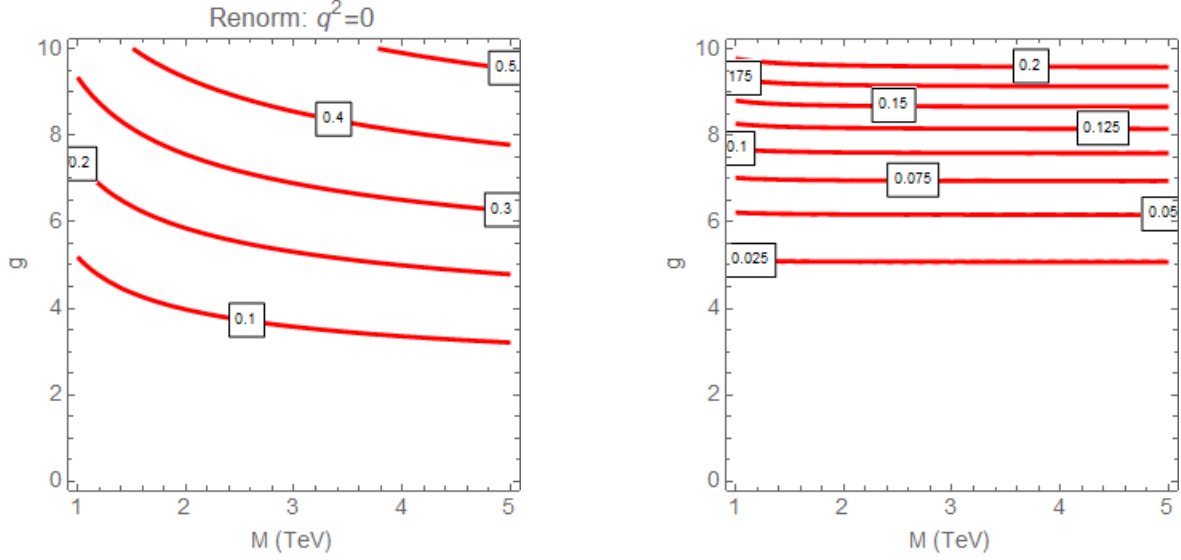


Figure 6: Contour lines of the parameter p for the $q^2 = 0$ scheme (left panel) and the $q^2 = M^2$ scheme (right panel).

In Fig. 6 we show contour lines for fixed values of the parameter p in the plane g and M in the $q^2 = 0$ scheme (left panel) and the $q^2 = M^2$ scheme (right panel). Three features appear distinctly:

- The dependence of p on M is mild, especially for the $q^2 = M^2$ renormalization scheme. For the $q^2 = 0$ the dependence is small but favoring the smaller values of M
- The main dependence of p appear on the renormalized gauge coupling, as expected. For values of $g = \mathcal{O}(1)$ it turns out that $p \ll 1$.
- Even for large values of g , $g = \mathcal{O}(10)$ the values of p are moderate: $p \simeq 0.5$ for the $q^2 = 0$ renormalization scheme, and $p \simeq 0.2$ for the $q^2 = M^2$ renormalization scheme.

In conclusion, we decide to continue the study of the Kaluza-Klein gluon at the renormalization scale $q^2 = M^2$, due to smaller values of p and a constant behaviour of the coupling constant.

⁸This study is outside the scope of the present work.

4 Production and decay of KK gluons: partonic level

In this section we compute, at the partonic level, the cross-section of a $2 \rightarrow 2$ process. We will consider the Drell-Yann production (induced by light quarks q) of the heavy KK gluon G , which decays into a pair of top right-handed quarks. We can for simplicity assume that only the channel $G \rightarrow \bar{t}_R t_R$ is available, as we are assuming the quark t_R is the only one localized in the extra dimension toward the IR brane. In the case that several quarks contribute to the G decay width, we have just to sum over the number of available final states. As we will see this generalization is trivial as the width depends only mildly on the quark mass, and this dependence can be safely neglected.

$$q\bar{q} \rightarrow G + g \rightarrow \bar{t}_R t_R$$

For a $2 \rightarrow 2$ process, the matrix element

$$i\mathcal{M}_{if} = \bar{v}(p')(-i\gamma^\alpha)\frac{(1-\gamma_5)}{2}u(p)iD_{\alpha\beta}(q)\bar{u}(k)(-i\gamma^\beta)v(k') \quad (4.1)$$

where $D_{\alpha\beta}(q)$ is a generalization of the propagator for the mediator. However, if we recall from Sec. 3 the propagator for the massive gluon for Feynman gauge plus the propagator of the gluon

$$\begin{aligned} D_{\alpha\beta}(q) &= (g_{\alpha\beta} - q_\alpha q_\beta / q^2) \left(\frac{1}{q^2} + \frac{1}{q^2 - M_R^2 - q^2 \widehat{\Pi}(q^2)} \right) \\ &\equiv (g_{\alpha\beta} - q_\alpha q_\beta / q^2) D(q). \end{aligned} \quad (4.2)$$

Since we are contracting the Lorentz structure with a current of fermions

$$\frac{q_\alpha q_\beta}{q^2} \bar{u}(k)(-i\gamma^\beta)v(k') = 0. \quad (4.3)$$

We now square the matrix element

$$\begin{aligned} |\mathcal{M}_{if}|^2 &= \frac{1}{4} |D(q)|^2 (\bar{v}(p')\gamma^\alpha(1-\gamma^5)u(p)g_{\alpha\beta}(q)\bar{u}(k)\gamma^\beta(1-\gamma^5)v(k')) \\ &\quad (\bar{v}(k')\gamma^\mu u(k)g_{\mu\nu}(q)\bar{u}(p)\gamma^\nu v(p')) \end{aligned} \quad (4.4)$$

Besides, we suppose the beams are unpolarized and we do not care about the final state spins. Thus, we have to average over two possible initial spins and sum over all the possible spins in the final state

$$|\mathcal{M}_{if}|^2 \rightarrow \frac{1}{4} \sum_{all\ spins} |\mathcal{M}_{if}|^2. \quad (4.5)$$

We proceed in the same way as in the computation of the loop reaching the following result

$$\begin{aligned} \frac{1}{4} \sum_{allspins} |\mathcal{M}_{if}|^2 = & 2|D(q)|^2 \left((p \cdot k)(p' \cdot k') + (p' \cdot k)(p \cdot k') - (p \cdot p')(k \cdot k') - m_q^2(p \cdot p') \right) \\ & + |D(q)|^2 \left((p' \cdot p) + m_t^2 \right) (2(k' \cdot k)) + 4m_q^2. \end{aligned} \quad (4.6)$$

We now continue the computation in the centre of mass reference frame. Hence, we can define the four-vectors of the particles involved

$$p = (E, p) \quad p' = (E, -p) \quad k = (E, k) \quad k' = (E, -k).$$

Doing some algebra the cross section is

$$\begin{aligned} \sigma = & \frac{g_s^4}{64\pi} s \left[1 + \frac{4}{s}(m_q^2 + m_t^2) + \frac{1}{3} \left(1 - \frac{4m_q^2}{s} \right) \left(1 - \frac{m_t^2}{s} \right) \right] \\ & \left[\frac{1}{s^2} + \frac{g_{t_R} g_q}{s(s - M^2 - s\widehat{\Pi}(s))^\dagger} + \frac{g_{t_R} g_q}{s^\dagger(s - M^2 - s\widehat{\Pi}(s))} + \frac{(g_{t_R} g_q)^2}{|s - M^2 - s\widehat{\Pi}(s)|^2} \right] \end{aligned} \quad (4.7)$$

We explained in Sec. 2.3 that the coupling constants depend on the localization of the field. As a first approximation we take the next quark flavours as "light" quarks ⁹:

$$q = u, d, s, c, b, t_L$$

These light quarks have a flat profile in the extra dimension, or they are localized toward the UV brane, while the Kaluza-Klein gluon is localized toward the IR brane. Thus, the coupling to the light quarks must be small. From the result in Fig. 3 (see also e.g. Refs. [9, 10]) we set $g_q = -0.2$. On the other hand, for the right handed top quark we vary the strength of the coupling constant, so as to see the effect in the process. In Fig. 7 we show the cross-section times branching ratio for $g_{t_R} = 8$ (left panel) and 3 (right panel) compared with the Standard Model. If the Extra dimensional theory were to be right we should be able to see a bump around the mass of the Kaluza-Klein gluon. We see that for bigger values of g_{t_R} the bump is wider, in other words, the decay width of the Kaluza-Klein gluon is bigger. We can connect this effect with the optical theorem where

$$\Gamma = M \text{Im} \left[\widehat{\Pi}(M) \right]. \quad (4.8)$$

⁹At this level considering that t_L is "light" means that t_L is not localized toward the IR brane, and thus interacts weakly with the KK gluon.

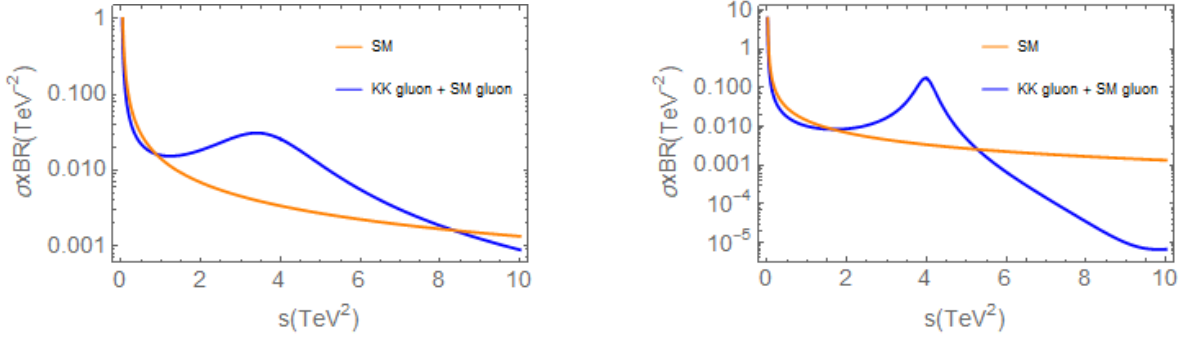


Figure 7: Cross-section times branching ratio Vs. center of mass momentum for Extra Dimensional Theory (for a G mass $M = 2$ TeV) and Standard Model. In the left panel $g_{t_R} = 8$. In the right panel $g_{t_R} = 3$. \sqrt{s} is the center of mass energy at the partonic level.

An effect that is also noticeable at big values of g_{t_R} is the displacement of the peak to the left. This is due to the first order correction in Sec. 3. The correction makes the mass of the Kaluza-Klein gluon smaller ($M_p < M$). An asymmetry also appears in the bump, which makes the tail of the cross-section longer.

As we already mentioned the bump is shifted to the left, so it will be interesting to compare the propagator in Eq. (3.6) with a simple Breit-Wigner approximation for the propagator, where

$$D_{BW}(s) = \frac{1}{s - M^2 - iM\Gamma}. \quad (4.9)$$

Hence, we substitute in Eq. (4.7) our propagator with the Breit-Wigner approximation

$$D(s) = \frac{1}{s - M^2 - s\hat{\Pi}(s)} \rightarrow D_{BW}(s).$$

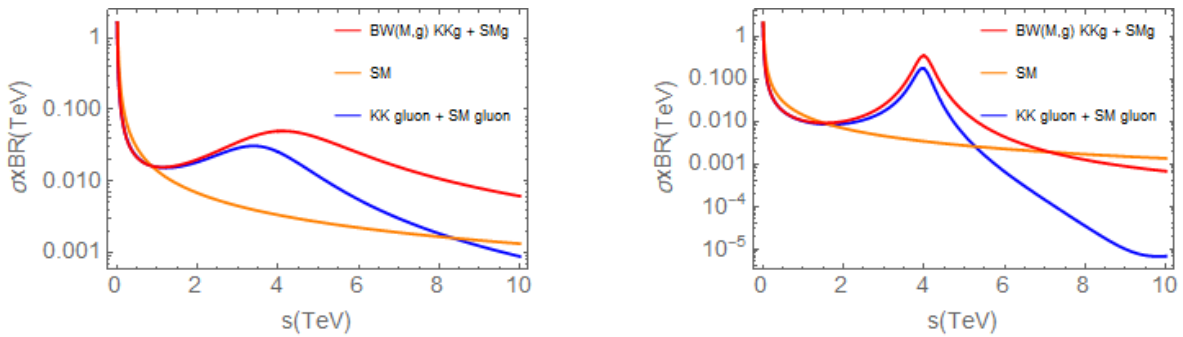


Figure 8: Comparison of the Breit-Wigner approximation and the computed propagator. In the left figure $g_{t_R} = 8$. In the right figure $g_{t_R} = 3$

In Fig.8 we see how the cross-section is affected by the choice of the propagator. For the Breit-Wigner approximation the cross-section is bigger in both cases: $g_{t_R} = 8$ and $g_{t_R} = 3$. For small values of the coupling constant we see that the peak is bigger for the Breit-Wigner approximation. However, at big values of g_{t_R} the peak is not shifted, $s = 4TeV^2$, unlike the case of the full propagator. Besides, the peak is symmetric as expected for the Breit-Wigner case. At high values of s the difference in the cross-section is still noticeable.

This effect needs to be taken into account in more detailed studies. For example when studying these processes with automated computation of differential cross-sections, such as MadGraph, where an introductory study is done in the next section.

5 KK gluons in proton-proton collisions

In order to have more precise and realistic results we should compute the cross section for proton-proton collisions. Since we can not scatter two free quarks due to QCD confinement, in order to find new physics, proton-proton colliders are used, such as the Large Hadron Collider (LHC) in Geneva. Nevertheless, this computation can not be carried out only theoretically because of the non-perturbative nature of the structure of the proton.

The cross-section in a proton-proton collision is symbolically defined as

$$\sigma_h = \int \underbrace{f_1 \otimes f_2}_{npQCD+pQCD} \otimes \underbrace{\hat{\sigma}_{parton}}_{pQCD}; \quad (5.1)$$

where the parton distribution functions (PDFs) are needed for each proton. Fortunately, the factorization theorem allows us to study the cross-section with perturbative and non-perturbative QCD, where σ_h is the hadronic cross-section, f_1 and f_2 the PDFs and $\hat{\sigma}_{parton}$ the partonic cross section, which we have already computed. The PDFs are treated perturbatively and non-perturbatively: pQCD and npQCD. The pQCD is treated with DGLAP (Dokshitzer-Gribov-Lipatov-Altarelli-Parisi) equations, that show us the probability of a parton to radiate. On the other hand, the npQCD has to be experimentally measured.

Thus, we are making use of MadGraph5_aMC@NLO [11] to compute the hadronic cross-section, σ_h . However, we need to generate a model for our Kaluza-Klein gluon.

5.1 Building the Kaluza-Klein gluon model

Here we are summarizing the process of building the model. We use FeynRules [12], a Mathematica-based package that, from the Lagrangian, calculates Feynman rules, to create the new model. Since the package has the Standard Model implemented, we only need to generate a small extension.

First, we define our Kaluza-Klein gluon G_μ^a as a $SU(3)_c$ massive gauge boson. However, unlike the Standard Model gluon g_μ^a , we need to define four different couplings, since the localizations of the quarks in the fifth dimension is not the same. This time we make a different and more precise approximation than in Sec. 4: $u, d, s, c \in q_{light}$. The coupling of the "light" quarks to the first mode Kaluza-Klein gluon is

$$q_{light} \rightarrow g_q = -0.2.$$

For the top and bottom quarks we differentiate their chiralities. The left handed top and bottom quarks will transform as a doublet. Thus, they have the same coupling

constant

$$t_L, b_L \rightarrow g_{t_L} = g_{b_L} = 1,$$

that it will take a non significant value. Lastly, the right handed top and bottom quarks that transform as singlets,

$$t_R \rightarrow g_{t_R} \quad \& \quad b_R \rightarrow g_{b_R}.$$

These coupling constants are going to be set later in the param-card in MadGraph, when running the program. Note that we only define the couplings for the quarks and not for the Standard Model gluon, as a result of the normalization of the Kaluza-Klein wave functions:

$$\int_0^L dy f_A^{(n)} f_A^{(m)} = L \delta_{n,m}. \quad (5.2)$$

The self coupling is also not considered because its effects can be neglected.

Now that we have defined the gauge group and the couplings to the Standard Model particles, we need to write the interaction Lagrangian, which is defined in Eq. (3.1). Then, we implement the new Lagrangian to the Standard Model Lagrangian and generate the vertices. Once this is done we compile it as an UFO file, the format that MadGraph works with.

5.2 Hadronic cross-section

Now that we created our extension of the Standard Model, we are studying the cross-section in the next process:

$$pp \rightarrow G + g \rightarrow t\bar{t}.$$

We find six different diagrams involving the Kaluza-Klein gluon. The scattering of two top quarks is neglected, since probability to find a top quark inside the proton is negligible. The rest of the processes computed are taken as background.

As mentioned before, the form of the propagator is important. MadGraph uses the Breit-Wigner approximation for the propagator of a resonance, thus we need to approximate our propagator to a Breit-Wigner form. We are using the pole mass and the pole decay width we can find in Eq. (3.23). In Fig. 9 we show a comparison between the different forms of propagators, using the approximations in Sec. 4. We see that at small values of g_{t_R} the Breit-Wigner form with M_p and Γ_p matches correctly our computation for the propagator. However, at large values of g_{t_R} the cross-section in the Breit-Wigner form with the pole parameters starts being bigger for $s > 2 \text{ TeV}^2$ and eventually the gap gets bigger in the tail. In all cases the difference between the

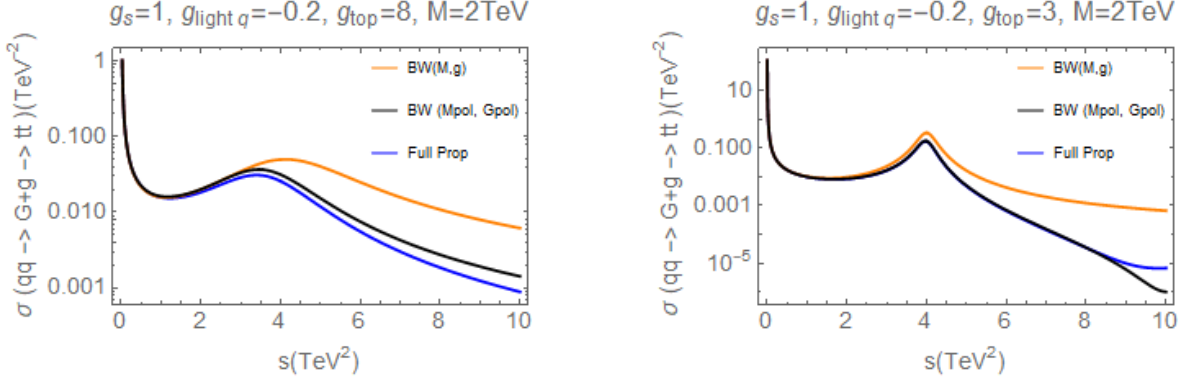


Figure 9: Comparison between partonic cross sections with different forms of propagators. In the left picture $g_{t_R} = 8$. In the right figure $g_{t_R} = 3$.

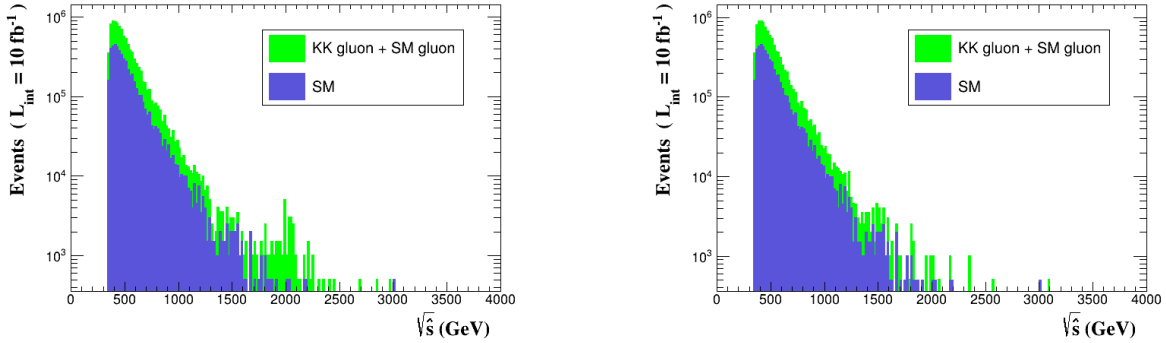


Figure 10: Comparison between Standard Model and Kaluza-Klein gluon for $pp \rightarrow t\bar{t}$ process at $\sqrt{s} = 13\text{TeV}$ and $M = 2\text{TeV}$. Left panel: $\Gamma = 0.1M$. Right panel: $\Gamma = 0.5M$.

cases $BW(M_p, \Gamma_p)$ and $BW(M, \Gamma)$ is remarkable and shows that when dealing with broad resonances it is important to keep track of these corrections.

Moreover the difference between using the $BW(M_p, \Gamma_p)$ approximation and the full propagator is tiny in all cases, and in any case the cross-section for $BW(M_p, \Gamma_p)$ can be at most a bit larger, only in extreme cases, than the cross-section using the full propagator. Therefore the comparison with experimental results using the approximation $BW(M_p, \Gamma_p)$ in MadGraph will yield conservative bounds. An analysis and comparison with present LHC data will be done in a separate publication [13].

In Fig. 10 we show a comparison between the Standard Model and Kaluza-Klein gluon for the $pp \rightarrow t\bar{t}$ process. For the left panel where we set a narrow decay width, we see that the cross-section increases by a small amount in the whole range of $\sqrt{\hat{s}}$. As expected, since it is a narrow decay width, a bump appears at $\sqrt{\hat{s}} = 2\text{ TeV}$ making the tail larger. For the right panel a wider decay width is set, $\Gamma = 1\text{ TeV}$. In this case the

cross-section also increases in the whole range of $\sqrt{\hat{s}}$. However, due to the decay width the bump vanishes. In addition, we can observe a larger tail.

6 Summary and outlook

We have studied and investigated the first Kaluza-Klein gluon mode starting from the Extra Dimensional theory with AdS_5 background. We also have reviewed the key points of the extra dimensional theory to get a glimpse on the nature and interactions of the massive gluon mode. The localization of the fields along the fifth dimension plays a key role in order to understand the interactions between particles, and we have seen that it is a way to understand the hierarchy problem of the masses. While the gauge boson KK modes have a localization determined by the theory, and the Higgs boson is localized toward the IR brane, as we saw in Sec. 2.3, fermions are not fixed. In particular there is a real parameter c , providing the five-dimensional Dirac mass, with which we can adjust the localization of every fermion fields. Thus heavy fermions tend to be localized toward the IR brane, so as the overlap of the wave function with the Higgs field wavefunction is big, whereas light fermions are localized toward the UV brane, with then a small overlap with the Higgs wave function.

Our main focus in this work was the first Kaluza-Klein gluon mode (G_μ^a), an excitation of the Standard Model gluon (g_μ^a). This excitation all features in common with the gluon, i.e. the same gauge group, but of course a different mass. Therefore, the fact that it is massive makes it to be localized toward the IR brane. Thus, the couplings of the KK gluon to the quarks are not universal, and the interactions with them are not vector-like. We find that the more massive the particle is (also right handed) the stronger is the coupling. As a consequence, in a first approximation and to simplify the analysis, we only considered the right handed top quark when computing the vacuum polarization for the Kaluza-Klein gluon. We assume that the left-handed top is not so strongly localized toward the IR brane, as its localization need to be the same as that of the left-handed bottom (by $SU(2)_L$ gauge invariance) which is much lighter a quark than the top quark. As a result we were able to make a small study of the perturbativity of the theory that helped us to choose a renormalization scheme where one-loop corrections are sort of minimized.

The fact that strongly coupled fermions to a vector like field makes it a broad resonance is a general feature. As this is the case in the model we are considering we have studied different methods to deal with different renormalization schemes for broad resonances leading to a departure between the renormalized values of (M, Γ) and the corresponding pole values (M_p, Γ_p) . This departure of course increases with the value of the coupling of the KK resonance to the fermions, which means that it increases with the value of the parameter Γ/M , and need to be taken into account in our analysis of broad resonances.

We then applied our computations for the partonic process

$$q\bar{q} \rightarrow G + g \rightarrow t\bar{t}.$$

Here we learnt how the partonic cross-section behaves for different values of the coupling of the KK gluon G to the right-handed top quark. For large values of the coupling, the decay width was large, so that in a real data analysis the signal will appear in the tail of our histograms. Besides, we also showed how the correction affected the shape of the bump, making it asymmetric and shifted to a lower mass.

When studying a more realistic case, such as, proton-proton collision, using automated computations, we saw the importance of choosing a good approximation of the propagator. In the best case scenario, the Breit-Wigner propagator for M_p and Γ_p , the cross-section is higher than was expected. Thus, for future analysis it is an effect that needs to be taken into account.

For the $pp \rightarrow G \rightarrow t\bar{t}$ process, the jets produced from top quarks are boosted due to the great mass of the Kaluza-Klein gluon. However, the process has considerable background events, making this channel difficult to work with. A way out is the study for four top decay. Even though the cross-section compared to the two top decay is smaller, the channel is almost background free. It is important to note that the experimental analyses concerning four top decays are in progress now [14].

The broad exploration of the first Kaluza-Klein gluon mode leads us to interesting and promising results. The next steps for these studies is compare our results with experimental data. On the one hand, the two top decay channel has already been studied, and thus data are available. Here we can see if we can loosen up experimental bounds, as only ratios of decay widths over masses in between 10 – 40% have been analyzed. On the other hand, the four top decay channel has not been fully explored yet. A more detailed analysis including the channels $pp \rightarrow G \rightarrow t\bar{t}$ and $pp \rightarrow G \rightarrow t\bar{t}t\bar{t}$, and comparison with experimental results, is in progress [13]. Moreover we can set a starting point in order to motivate future experimental studies in the Extra dimensional theory.

References

- [1] T. Kaluza, *Zum Unitatsproblem der Physik*, *Sitzungsber. Preuss. Akad. Wiss. Berlin (Math. Phys.)* **1921** (1921) 966–972, [[arXiv:1803.08616](#)]. [Int. J. Mod. Phys.D27,no.14,1870001(2018)].
- [2] O. Klein, *Quantum Theory and Five-Dimensional Theory of Relativity. (In German and English)*, *Z. Phys.* **37** (1926) 895–906. [,76(1926)].
- [3] L. Randall and R. Sundrum, *A Large mass hierarchy from a small extra dimension*, *Phys. Rev. Lett.* **83** (1999) 3370–3373, [[hep-ph/9905221](#)].
- [4] W. D. Goldberger and M. B. Wise, *Modulus stabilization with bulk fields*, *Phys. Rev. Lett.* **83** (1999) 4922–4925, [[hep-ph/9907447](#)].
- [5] K. Agashe, A. Delgado, M. J. May, and R. Sundrum, *RS1, custodial isospin and precision tests*, *JHEP* **08** (2003) 050, [[hep-ph/0308036](#)].
- [6] K. Agashe, R. Contino, and A. Pomarol, *The Minimal composite Higgs model*, *Nucl. Phys.* **B719** (2005) 165–187, [[hep-ph/0412089](#)].
- [7] E. Ponton, *TASI 2011: Four Lectures on TeV Scale Extra Dimensions*, in *The Dark Secrets of the Terascale: Proceedings, TASI 2011, Boulder, Colorado, USA, Jun 6 - Jul 11, 2011*, pp. 283–374, 2013. [arXiv:1207.3827](#).
- [8] M. Quiros, *Higgs Bosons in Extra Dimensions*, *Mod. Phys. Lett.* **A30** (2015), no. 15 1540012, [[arXiv:1311.2824](#)].
- [9] B. Lillie, L. Randall, and L.-T. Wang, *The Bulk RS KK-gluon at the LHC*, *JHEP* **09** (2007) 074, [[hep-ph/0701166](#)].
- [10] R. Barcelo, A. Carmona, M. Masip, and J. Santiago, *Gluon excitations in t \bar{t} production at hadron colliders*, *Phys. Rev.* **D84** (2011) 014024, [[arXiv:1105.3333](#)].
- [11] J. Alwall, R. Frederix, S. Frixione, V. Hirschi, F. Maltoni, O. Mattelaer, H. S. Shao, T. Stelzer, P. Torrielli, and M. Zaro, *The automated computation of tree-level and next-to-leading order differential cross sections, and their matching to parton shower simulations*, *JHEP* **07** (2014) 079, [[arXiv:1405.0301](#)].
- [12] A. Alloul, N. D. Christensen, C. Degrande, C. Duhr, and B. Fuks, *FeynRules 2.0 - A complete toolbox for tree-level phenomenology*, *Comput. Phys. Commun.* **185** (2014) 2250–2300, [[arXiv:1310.1921](#)].
- [13] R. Escribano, M. Mendizabal, and M. Quiros [in preparation](#).
- [14] **ATLAS** Collaboration, M. Aaboud et al., *Search for four-top-quark production in the single-lepton and opposite-sign dilepton final states in pp collisions at $\sqrt{s} = 13$ TeV with the ATLAS detector*, *Phys. Rev.* **D99** (2019), no. 5 052009, [[arXiv:1811.02305](#)].